Macromolecular Materials and Engineering
Open Access
www.mame-journal.de

Rationalizing the Effect of the MAA/PEGMA Ratio of Comb-Shape Copolymers Synthetized by Aqueous Free-Radical Copolymerization in the Hydration Kinetics of Ordinary Portland Cements

Sara Beldarrain, Aitor Barquero, Guido Goracci, Jorge S. Dolado, and Jose Ramon Leiza**

Methacrylic acid-co-poly(ethylene glycol methacrylate) (MAA-co-PEGMA) copolymers (MPEG-type polycarboxylate ether (PCE) superplasticizers) are characterized by a comb-like structure. Although they have been used for years as dispersants in cementitious formulations, their structure–property relationship is still not fully understood. In this work, PCEs with uniform composition and different charge-density (*N*) or different side chain lengths (*P*) are synthesized by free-radical copolymerization varying the MAA/PEGMA ratios and ethylene oxide units in the PEGMA macromonomers. The effect of these copolymers on the hydration kinetics of an Ordinary Portland Cement (OPC) is analyzed, and it is observed that by increasing the PCE concentration the hydration is delayed. For a given PCE concentration, the delay is longer as the MAA/PEGMA ratio increases or the side chain length of the PEGMA decreases. The hydration delay is proportional to the carboxylate dosage and all PCEs fit in a master curve proving that the microstructure of the PCEs synthesized by free-radical copolymerization can be correlated with the hydration delay of a commercial OPC.

1. Introduction

It is fair to say that nowadays concrete technology progresses in parallel to the development of modern Polycarboxylate ether/ester (PCE) polymers. PCEs represent the latest family of superplasticizers which, due to their superior water-reducing ability, have replaced former chemistries based on lignosulfonates (LS), polynaphthalene sulfonates (PNS), or polymelamine sulfonate (PMS).[1] PCEs are comb-like structures with a backbone formed by anionic carboxylic groups and non-ionic polyethylene glycol (PEG) units as pendant groups (side chain) (**Figure 1**a). Their molecular versatility, manifested by the multiple structures that can be formed just by changing parameters like the chemistry or length of the backbone, the number and length of the side chains, etc., allows for achieving good workability even at very low water-to-binder ratios. This explains why PCEs are essential ingredients of advanced formulations of concrete, including ultra-high strength concrete (UHPC)[2] or self-compacting concrete (SCC).[3]

In spite of their wide use, our understanding on the PCE's performance has largely relied on a trial and error approach until very recently. Fortunately, a set of pioneering works has enabled to rationalize the performance of PCEs based on their structural topology. In this regard and with the aim of understanding the microstructure-property relationship of comb-like PCEs, Flatt et al.[4] characterized the microstructure of comb-like PCE's by defining a model repeating unit (see Figure 1b), which can be fully described by three characteristic structural parameters, which are the number of monomer units in the repeating unit of the backbone chain, *N*, the number of ethylene glycol units in the side chains, *P*, and the number of repeating units in the chain, *n*.

Interestingly, an unprecedented insight on the interaction between the cement surfaces and PCEs was possible from this novel approach. For instance, the absorbed conformation of the comb-like polymers tuned out to be well described in terms of scaling laws.[4] Likewise, the posterior work of Marchon et al.[5] tackled the tantalizing challenge of explaining why organic admixtures can cause a retardation of cement hydration. In particular, their work deeply analyzed the impact of a PCE on a specially designed model cement and proposed master curves capable of linking the cement hydration delay with dosages and molecular structure parameters. This outcome opened the path for a better understanding of structure–properties relationship, which can later be used for a custom design of PCEs to achieve the desired performance.

S. Beldarrain, A. Barquero, J. R. Leiza
POLYMAT, Kimika Aplikatua Saila, Kimika Falkultatea
University of the Basque Country
UPV/EHU, Joxe Mari Korta Zentroa, Tolosa Hiribidea 72, Donostia-San Sebastián 20018, Spain
E-mail: jrleiza@ehu.eus

G. Goracci, J. S. Dolado
Centro de Física de Materiales (CSIC, UPV/EHU) Materials Physics Center (MPC) Paseo Manuel de Lardizabal 5
Donostia-San Sebastián 20018, Spain
E-mail: jorge_dolado002@ehu.eus

DOI: 10.1002/mame.202300032

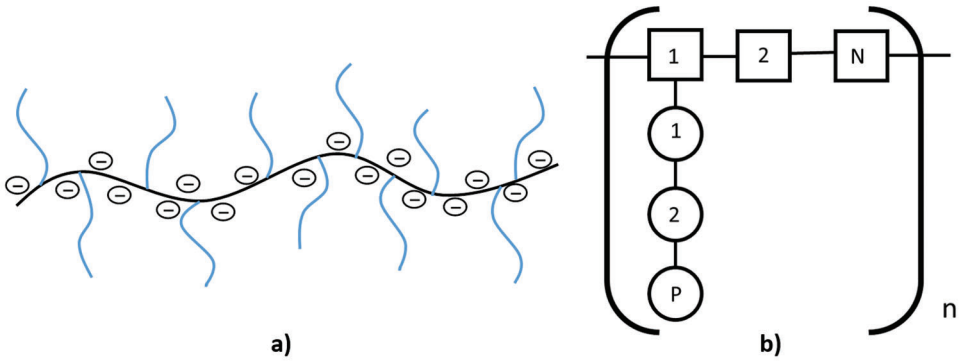

Figure 1. a,b) Schematic illustration of typical PCE structure and the repeating unit of a comb-shaped copolymer considered by Flatt et al.[4] The comb copolymer contains *n* segments, each containing N backbone monomers and a side chain of P ethylene oxide units.

In this context, this paper aims to extend our understanding on the influence of PCEs on cement hydration delay. To this end, PCEs with controlled topology have been synthesized by free-radical polymerization and their impact on the hydration of a commercial OPC has been carefully analyzed. Though these copolymers have been added to a commercial OPC through a direct addition method, the experiments reveal that the hydration delay is proportional to the carboxylate dosage and can be effectively displayed in master curves, as proposed by Marchon et al.[5]

2. Experimental Section

2.1. Materials

Methacrylic acid (MAA), 99.5% with 250 ppm monomethyl ether hydroquinone (MEHQ) as inhibitor was purchased from Acros Organics, polyethylene glycol methyl ether methacrylates (PEGMA) with 22.5 and 45 ethylene glycol units (average Mn: 1000 and 2000 g mol^{-1}, respectively) with 200 ppm MEHQ as inhibitor, and 50 wt.% water solution was kindly supplied by Evonik Industries. 3-mercaptopropionic acid (3-MPA), potassium persulfate (KPS), sodium bicarbonate ($NaHCO_3$), sodium nitrate ($NaNO_3$), and sodium hydroxide (NaOH) were purchased from Sigma–Aldrich and used as received. Deionized water was employed as solvent. Chromatography grade N-N-dimethylformamide (DMF) from Fisher–Scientific was used as internal reference in ^{1}H-NMR experiments and deuterium oxide (D_2O) purchased from Deutero and used as cosolvent for ^{1}H-NMR and ^{13}C-NMR. The cement used was CEM type I 52.2R Ordinary Portland Cement (OPC), which was kindly supplied by Lemona Cements S.A. Its mineralogical composition, determined by X-ray diffraction (BRUKER D8 Advance) using Rietveld refinement, is shown in **Table 1**. Its specific surface area calculated according to Blaine fineness method (UNE EN 196-6:2010) was 0.4523 m^2 g^{-1}.

Table 1. Mineralogical composition of the Ordinary Portland Cement type I 52.5R obtained by XRD and Rietveld refinement.

Rietveld Analysis	
Phases	wt.%
Amorphous	10.8
C_3S	48.1
β-C_2S	17
Cubic C_3A	6.8
C_4AF	5.9
Calcite	6.1
Akermanite	2.1
Portlandite	1
Gypsum	0.9
Quartz	0.6
Bassanite	0.6
Dolomite	–

2.2. Synthesis of the PCEs

The copolymerization reactions were carried out in aqueous solution in semibatch in a 250 mL glass jacketed reactor with a thermostatic water bath and a mechanical turbine stirrer at 200 rpm. The reactor lid was equipped with a feeding inlet, a condenser, nitrogen bubbling, and a sampling device.

To carry out the reactions, deionized water (100 g) was loaded to the reactor and heated to 80 °C. During the heating, the system was purged using a nitrogen flow at 15 mL min^{-1}. The nitrogen flow was maintained during the reaction. When the reaction temperature was achieved, the feeding started. The monomers (PEGMA and MAA), initiator (KPS), and sodium bicarbonate dissolved in the rest of the water (see Table 3) were fed in the same stream for 3 h at 0.56 g min^{-1}. After, post polymerization was carried out for 1 h, with the aim of reaching full conversion of the monomer. The solids content (SC) and amount of chain transfer agent (CTA) varied depending on the reaction in order to control viscosity during the reaction. **Table 2** summarizes the PEGMA type, MAA/PEGMA ratio, final solids content, and CTA amount for each PCE that was synthetized.

During the reaction, five aliquot samples of ≈2 mL were taken to calculate the monomer conversion. A couple of drops of hydroquinone (1 wt.% aqueous solution) were added to the samples and immersed in an ice bath, to stop the polymerization. **Table 3** presents the formulation used in the synthesis of the copolymers.

Table 2. Characteristics of the synthesized copolymers.

PCE	Macromonomer	MAA/PEGMA [mol mol^{-1}]	SC [%]	CTA [% wbm]
0.67/1 M	PEGMA22.5	0.67/1	*20*	*0*
1/1 M		1/1	*20*	*0*
3/1 M		3/1	20	*0*
6/1 M		6/1	*10*	*0*
0.67/1 L	PEGMA45	0.67/1	*10*	*0.5*
1/1 L		1/1	*10*	*0.5*
3/1 L		3/1	*5*	*0.5*
6/1 L		6/1	*5*	*0.5*

Table 3. Formulation to synthesize the copolymers.

PCE	Initial charge [g]	Feeding [g]					
	Water	MAA	PEGMA	Water	KPS	$NaHCO_3$	3-MPA
0.67/1 M	100	3.25	113.5	33.3	1.2	0.36	0
1/1 M	100	4.75	110.5	34.8	1.2	0.36	0
3/1 M	100	12.3	95.4	42.3	1.2	0.36	0
6/1 M	100	10.21	39.6	100.2	0.6	0.18	0
0.67/1 L	100	0.84	58.33	90.8	0.6	0.18	0.15
1/1 L	100	1.24	57.53	91.2	0.6	0.18	0.15
3/1 L	100	1.71	26.57	121.7	0.3	0.09	0.08
6/1 L	100	3.08	23.85	123.1	0.3	0.09	0.08

2.3. Characterization of the PCEs

The individual conversion of each monomer was calculated using ^{1}H-NMR. A couple of drops (≈45 mg) of DMF were added to the vial as an internal reference. Five hundred microliters of solution were taken and transferred together with 100 µL of D_2O to an NMR tube. Spectra were recorded by employing Watergate sequence in a Bruker AVANCE 400 MHz equipment.[6] The Watergate sequence aims at removing the water resonance from the spectra using a sequence of pulse trains with five pairs of symmetric pulses (W5) to enhance the signal of the peaks of interest, which are the two monomers. The conversion of MAA and PEGMA was calculated from the evolution of the peaks corresponding to the vinyl protons of MAA (δ = 5.60 and 5.25 ppm) and PEGMA (δ = 6.10 and 5.70 ppm). The instantaneous (Equation 1) and global conversion (Equation 2) of each monomer and the cumulative copolymer composition (Equation 3) were calculated from the amount of unreacted monomer as follows:

$$x_i^{\text{inst}} = 1 - \frac{\frac{A_i}{2} \cdot n_{\text{DMF}}/A_{\text{DMF}}}{F_i \cdot t/Mw_i} \tag{1}$$

$$x_i^{\text{glob}} = \frac{F_i \cdot t/Mw_i - \frac{A_i}{2} \cdot n_{\text{DMF}}/A_{\text{DMF}}}{F_i \cdot t_{\text{final}}/Mw_i} \tag{2}$$

$$Y_{\text{MAA}} = \frac{F_{\text{MAA}} \cdot t \cdot x_{\text{MAA}}^{\text{inst}}}{F_{\text{MAA}} \cdot t \cdot x_{\text{MAA}}^{\text{inst}} + F_{\text{PEGMA}} \cdot t \cdot x_{\text{PEGMA}}^{\text{inst}}} \tag{3}$$

where A_i is the area of MAA or PEGMA monomers, A_{DMF} is the area of DMF (δ = 7.9 ppm), n_{DMF} is the amount of DMF in mol, t is the reaction time in minutes, Mw_i is the molar mass of MAA or PEGMA in g mol^{-1}, F_i is the feeding rate in g min^{-1} of MAA or PEGMA, and $x_{\text{MAA}}^{\text{inst}}$ and $x_{\text{PEGMA}}^{\text{inst}}$ the instantaneous conversions of MAA and PEGMA monomers, respectively.

The monomer sequence distribution of one of the copolymers was determined by a Gaussian/Lorentzian deconvolution of the carbonyl peaks of MAA in ^{13}C-NMR spectroscopy using Mestre–Nova software (version 11.0.4) as presented elsewhere.[7] The Spectrum was taken in a Bruker AVANCE 500 MHz equipment. Five hundred microliters of the sample were taken and mixed with 100 µL of D_2O in a NMR tube. The acquisition time of the experiment was 9 h with 7000 scans.

Due to the high intensity of the ethylene glycol peak, the spectra were recorded with a selected pulse from 170 to 200 ppm, thus, the intensity of this region is intensified. Two different signals appear; one corresponds to the acid comonomer and the other to the ester one. Due to the high concentration of the acid comonomer, its signal is more intense. Therefore, deconvolution was made based on the acid signal. The theoretical values were calculated based on the Bernouillian distribution, which was based on the experimental copolymer cumulative composition determined as described in Section 2.3. The spectrum was well enough resolved to perform deconvolution in triads (A is MAA and B is PEGMA). The comparison between theoretical and experimental values provides information on the homogeneity of the composition of the copolymers obtained. Equation 4 was employed for the theoretical calculation of the triads, where Y_{MAA} is the cumulative composition of the copolymer with respect to MAA.

$$\begin{aligned}(AAA) &= {Y_{MAA}}^3 \\ (AAB) &= {Y_{MAA}}^2 \cdot (1 - Y_{MAA}) \\ (BAB) &= (1 - Y_{MAA})^2 \cdot Y_{MAA}\end{aligned} \tag{4}$$

The molar mass distribution of the polymers was analyzed by Asymmetric-Flow Field-Flow Fractionation with Multi Angle Light Scattering and Refractive Index detectors (AF4/MALS/RI). Separation was carried out on a 27.5 cm trapezoidal channel mounted on PEEK (polyether ether ketone). The channel thickness spacer was 350 µm. The accumulation wall was a regenerated cellulose membrane with a cut-off molar mass of 10000 Da. AF4 flow control was maintained with a Wyatt Eclipse 3 AF4 Separation System controller, the MALS detector was a miniDAWN Treos multiangle (3 angles) and the RI detector was an Optilab T-Rex differential refractometer (658 nm), all from Wyatt Technology Corp., USA.

The analyses were carried out at 35°C and a $NaNO_3$ 0.1 mol·L^{-1}, pH = 10 (using NaOH as base) aqueous solution was used as eluent. Copolymer solutions with a concentration of 10 mg·mL^{-1} were prepared and injected (50 µL) into the equipment, except for copolymer 3/1 L, in which 75 µL were injected, and 6/1 L copolymer, in which a solution with a concentration of 15 mg·mL^{-1} was prepared. The AF4/MALS/RI data was analyzed by using the ASTRA software version 6.1 (Wyatt technology, USA). The absolute molar masses were calculated from the MALS/RI data using the Debye plot (with first-order Zimm formalism). The

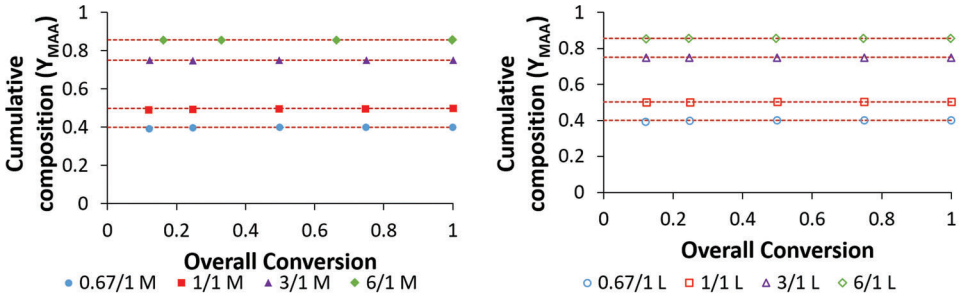

Figure 2. Conversionevolution of the cumulative copolymer composition referred to MAA comonomer. The dotted lines correspond to the composition of the feed. The figure on the left belongs to the short PEGMA (22.5 EO units) while the one on the right belongs to long PEGMA (45 EO units).

$dn \cdot dc^{-1}$ of each copolymer was measured, as reported in the Supporting Information (Section 1).

The value of the side chain length, *P*, was specified by the supplier. In addition, these macromonomers were analyzed by MALDI-TOF and confirmed the supplier's value (the spectra can be found in Figure S1, Supporting Information). The *N* value was calculated from the MAA/PEGMA mol ratio used in the formulation, also named C/E (N = MAA/PEGMA + 1) as it was confirmed that random and homogeneous copolymers with composition equal to the feed were produced during the polymerization (see Section 3.1). The number of repeating units, *n*, is defined as the number-average degree of polymerization (DP_n, obtained from the AF4/MALS/RI) divided by the number of monomers per segment (*N*).

2.4. Characterization of OPC

The hydration kinetics were carried out using a TAM air conduction calorimeter at room temperature for 48 h with water as reference material. Cement pastes with a total mass of 5 g were prepared with a 0.4 water to cement ratio. The mixing of the components was made by a vortex mixer with the following procedure: 90 s at 800 rpm, 60 s of pause and 90 s at 800 rpm. Figure S5 (Supporting Information) shows three repetitions of the hydration of a neat OPC (without PCE) to show the reproducibility of the experiments.

Calorimetric analyses examined the effect of different superplasticizers with different copolymer composition (*C/E* + 1 or *N*) and side chain length (*P*) at different concentrations (between 0.5 and 4 $mg_{PCE} \cdot g_{OPC}^{-1}$). The PCE was added dissolved in the initial water, using a method known as direct addition.

The evolution of the specific BET surface and X-ray Diffractogram (XRD) of the OPC was studied during cement hydration in absence and presence of PCE (in direct addition). For these measurements, 3/1 M PCE was used at 2 $mg_{PCE} \cdot g_{OPC}^{-1}$ concentration and at a 0.4 water to cement ratio and the same mixing procedure as in Section 2.4 was used. The hydrations were stopped at 30 min by the addition of cold isopropanol (5 °C) in a ratio of 12.5 $mL \cdot g_{OPC}^{-1}$. The pastes were mixed for 1 min before they were filtered using a Buchner funnel and dried in vacuum at 35 °C overnight.

The specific surface area of OPCs hydrated for 30 min without any PCE and in presence of PCEs were analyzed using a BET nitrogen physisorption device (Micrometrics). The samples were previously degasified for 16 h at 40 °C. The same samples were also analyzed by XRD (BRUKER D8 Advance X-Ray diffractometer with Cu Kα (λ = 1.5418 Å) radiation) in order to analyze ettringite formation.

Table 4. The ideal triads were calculated using the Bernoullian model for random copolymers (Equation 4) and the experimental triads by integrating the ^{13}C NMR spectrum from Figure S4 (Supporting Information).

Triad	Experimental	Ideal
(AAA)	0.442	0.422
(AAB)	0.298	0.281
(BAB)	0.010	0.046

3. Results and Discussion

3.1. Determination of the Microstructure of Comb-Shaped PCE's

The instantaneous conversions measured in all experiments were high, calculated from ^1H-NMR measurements (a representative ^1H-NMR is presented in Figure S2, Supporting Information), as shown in Figure S3 (Supporting Information).

The cumulative copolymer composition was determined with Equation 3 using the instantaneous conversions of each monomer. **Figure 2** shows the evolution of the cumulative copolymer composition over conversion, referred to MAA.

Figure 2 shows that homogeneous copolymer compositions were obtained in all experiments, namely, the composition was constant during the reaction and equal to the composition of the feed. This was achieved because the copolymerization reactions were carried out in acidic conditions, where the reactivity ratios of both monomers take an approximate value of 1 (r_{MAA} = 1.02; r_{PEGMA} = 1.03)[8] and due to the high instantaneous conversions achieved during the polymerization.

The monomer sequence distribution of a representative copolymer (1/3 M) was measured by ^{13}C NMR as described in the Experimental Section and elsewhere.[7] The fraction of triads calculated from the NMR analysis was compared with the theoretical triads distribution corresponding to an ideal copolymer (see **Table 4**). The ^{13}C NMR spectra are presented in Figure S4 (Supporting Information). The excellent agreement between the experimental and theoretical predictions (note that the error of the minor triad BAB is larger than that of the two main

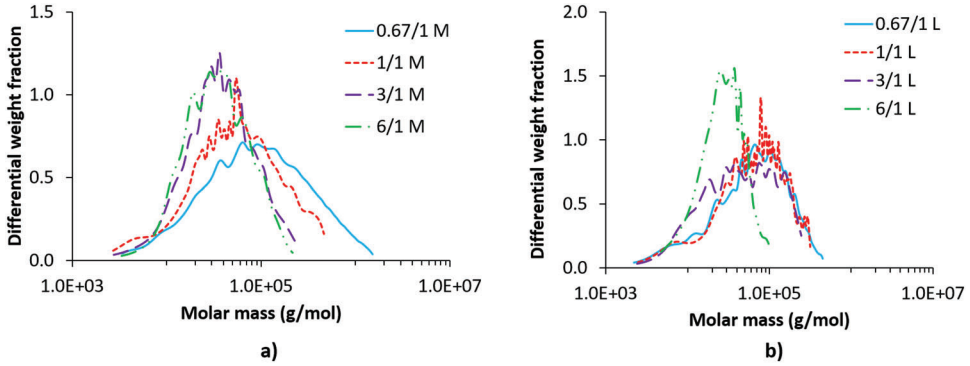

Figure 3. a,b) Molar mass distributions of the copolymers of series M and series L.

Table 5. Molecular characteristics of the synthesized PCEs.

PCE	$\overline{M_n}$ [kg mol^{-1}]	Đ	n_n
0.67/1 M	40.5 ± 3.8	4.4	38
1/1 M	27.6 ± 3.3	3.2	25
3/1 M	24.4 ± 2.0	2.0	19
6/1 M	24.5 ± 1.3	1.8	16
0.67/1 L	27.2 ± 2.6	3.3	13
1/1 L	29.0 ± 3.0	2.8	14
3/1 L	20.5 ± 1.4	3.0	9
6/1 L	17.2 ± 0.1	1.6	7

triads because of its smaller amount, which is more affected by the deconvolution analysis of the peaks) confirms that homogeneous and random copolymer chains with the desired composition were produced. Therefore, we can safely assume that the MAA/PEGMA ratio used in the feed can be used to determine the value *N* of the ideal repeating unit of a comb-shaped copolymer.

Molar masses and molar mass distributions of the copolymers synthesized by free-radical copolymerization were analyzed by AF4/MALS/RI. The exact dn dc^{-1} values were also calculated using the refraction index detector for the accurate molar masses determination,[7] as shown in Table S1 (Supporting Information).

Table 5 shows the molecular characteristics of the synthesized copolymers, while **Figure 3** shows the molar mass distributions for M and L series, respectively. DP_n is calculated from $\overline{M_n}$ using an average molar mass of the repeating unit (RU) based on the copolymer composition of each experiment. RU can be defined as $f_{MAA} \cdot Mw_{MAA} + f_{PEGMA} \cdot Mw_{PEGMA}$, where f_{MAA} and f_{MAA} are the molar fraction of each monomer, Mw_{MAA}. And Mw_{PEGMA} are the molar mass of MAA and PGMA monomers, respectively.

Molar masses for the copolymers synthesized with the shorter PEGMA (series M) were higher than the molar masses of the copolymers with the longest PEGMA. In the former series chain transfer agent (CTA) was not used and additionally higher solids content were targeted explaining the higher values for this series.

Also worth noting is that the degree of polymerization (DP_n), the average number of monomer units in the chains, is higher for the PCEs with shorter PEGMA and that increasing the MAA/PEGMA ratio the DP_n increases.

The conformation in solution of the PCE's synthesized in this work was determined by plotting $log(n) \cdot log(N)^{-1}$ versus $log(P) \cdot log(N)^{-1}$ for all the copolymers in the phase diagram defined by Gay and Raphael.[9] **Figure 4** shows the diagram where the points correspond to each of the copolymers.

It can be seen that the copolymers with the highest MAA/PEGMA ratios (3/1 and 6/1) show a flexible backbone worm (FBW) conformation, while the copolymers containing a higher side chain density show a stretched backbone, either worm (SBW), or star (SBS) conformation, regardless of the PEGMA used.

3.2. Hydration Kinetics

The PCEs were mixed with water (direct addition) and added to cement for the measurements of hydration kinetics. The effects of the molecular parameters of the PCEs (copolymer composition (*N*), concentration (dosage), and side chain length (*P*)) on the hydration kinetics were analyzed.

3.2.1. Effect of the PCE Concentration

Figure 5 shows the effect of the PCE concentration on the hydration kinetics of the OPC in direct addition for a PCE with a MAA/PEGMA (*N*) = 3/1 and *P* = 22.5. All the PCEs synthetized in this work show the same trend on the hydration kinetics (the additional results can be found in Figure S5, Supporting Information). The curve of the hydration of the OPC without any PCE is included in all figures as reference.

Contrary to what was reported by Marchon et al.[5] for direct addition, we observed a delay on the hydration of the silicate peak at all dosages of the PCE. Nonetheless, it can be observed that the effect is more pronounced at concentrations >1 mg g^{-1} OPC; somehow in partial agreement with the observation of Marchon et al., that below a critical concentration of the PCE the impact on the delay is limited, but in our results it is not negligible.

3.2.2. Effect of the MAA/PEGMA Ratio of the PCE (N)

Figure 6 shows the hydration kinetics of the OPC with the PCE of series M (*P* = 22.5) at different dosages of PCE for different

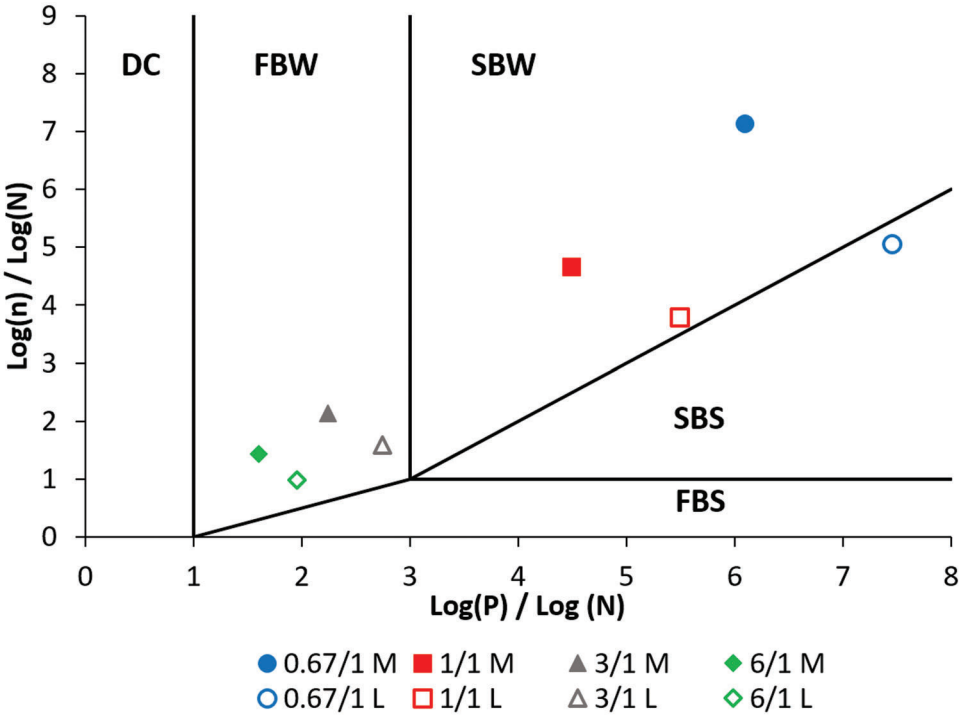

Figure 4. Conformation diagram for the synthesized comb copolymers with different MAA/PEGMA ratio.

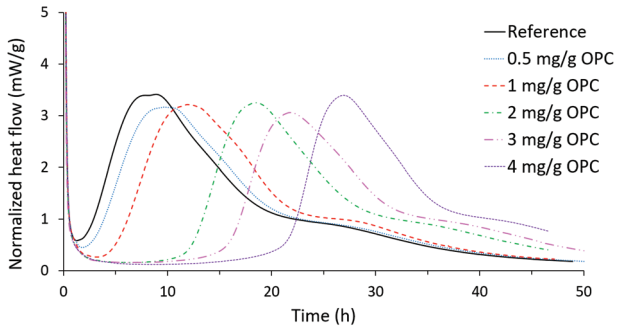

Figure 5. Effect of the PCE concentration at 3/1 MAA/PEGMA ratio and P = 22.5.

MAA/PEGMA ratios (*N*). On one hand, as shown in Figure 5, the higher the concentration of PCE, the higher the delay in the hydration, independent of the MAA/PEGMA ratio (*N*). However, at high PCE concentrations (>2 mg_{PCE} g_{OPC}^{-1}) the hydration delay increases with the MAA/PEGMA ratio. Interestingly, at low PCE concentrations (<1 mg_{PCE} g_{OPC}^{-1}), all the PCEs have the same effect regardless the MAA/PEGMA ratio. The same trend is observed for series L (see Figure S6, Supporting Information).

3.2.3. Effect of the Side Chain Length of PEGMA (P)

Figure 7 shows the effect of the side chain length (*P*) in the hydration curves for a given PCE dosage and MAA/PEGMA ratio of the PCE (3/1 MAA/PEGMA ratio and dosage of 3 mg g^{-1}). As observed, the copolymer of a shorter side chain presents a greater delaying effect than the one with a longer side chain (the same effect was found for the other PCE's that are presented in Figure S7, Supporting Information).

This might happen because for the same PCE dosage, the copolymer with a shorter lateral chain has a greater molar concentration of carboxylate groups, and as it was discussed in Sections 3.2.1 and 3.2.2. This enhances the delaying effect of the PCE.

3.2.4. Correlation Of the Hydration Delay with the Microstructure of the PCEs

The group of Flatt has pioneered the research to rationalize the effect of the molecular structure of comb-shaped copolymers (so-called superplasticizers) in the properties of cement pastes (rheology and hydration among others).[4,5,10–14] In the work of Marchon et al.,[5] the authors deeply analyzed the effect of comb-shaped copolymers prepared by transesterification of a poly(methacrylic acid) backbone with PEG of different lengths on the hydration kinetics of model cement pastes that contained a model clinker (80.9 wt.% tricalcium silicate, 17.2 wt.% tricalcium aluminate, and 2 wt.% of impurities including dicalcium silicate, quartz, and calcium oxide) plus 5 wt.% of hemihydrate. The authors analyzed the effect of the PCEs in the kinetics of hydration by calorimetric measurements using two addition modes for the PCE: delayed addition and direct addition; namely, the PCE was added 5 min after the cement paste was formed in delayed addition or it was directly incorporated into the water before the mixing in direct addition.

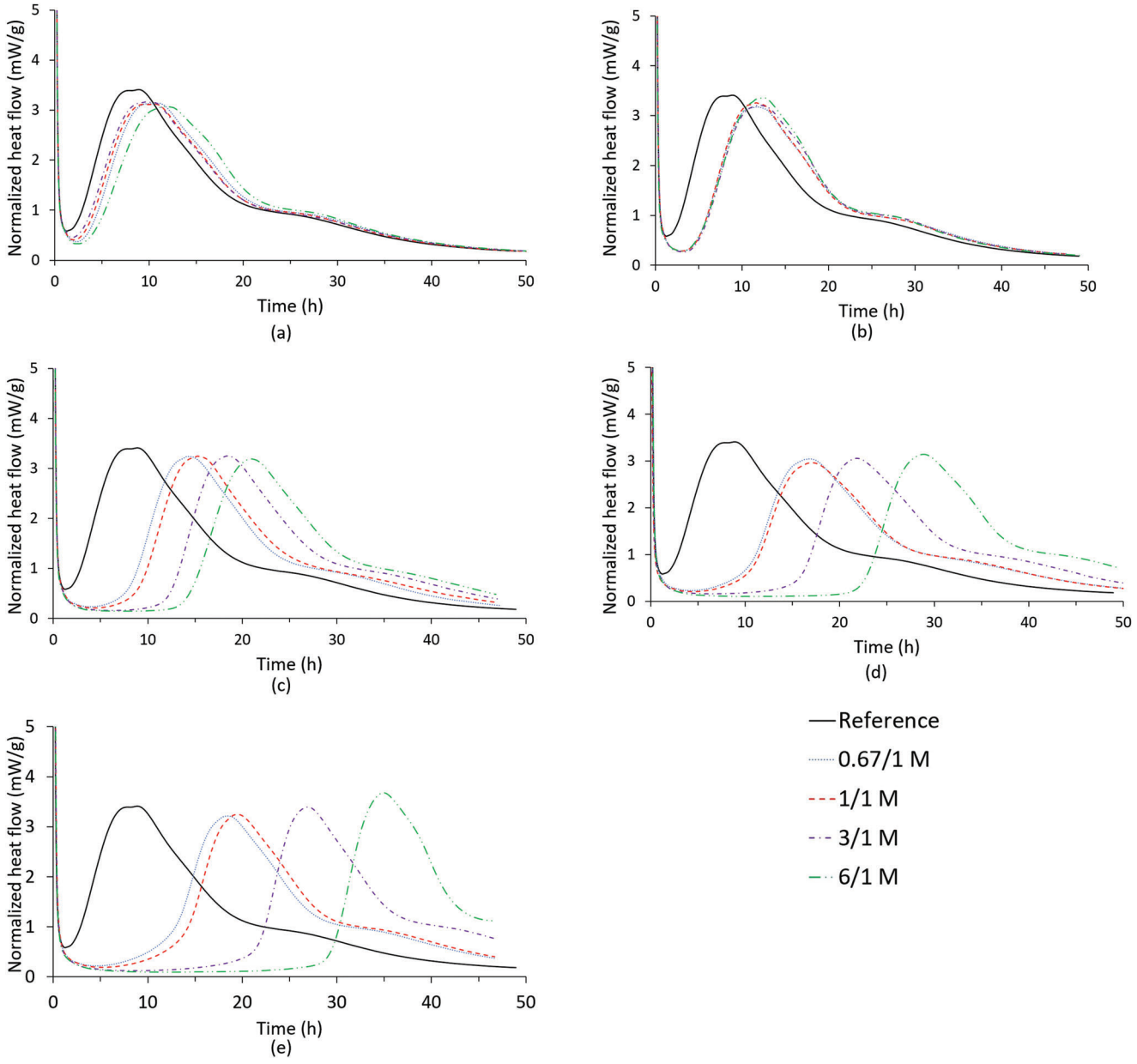

Figure 6. Effect of the copolymer composition of series M (P = 22.5) at different PCE concentrations: a) 0.5 $mg_{PCE}\ g_{OPC}{}^{-1}$, b) 1 $mg_{PCE} \cdot g_{OPC}{}^{-1}$, c) 2 $mg_{PCE}\ g_{OPC}{}^{-1}$, d) 3 $mg_{PCE}\ g_{OPC}{}^{-1}$, and e) 4 $mg_{PCE}\ g_{OPC}{}^{-1}$.

The authors found that the hydration retardation caused by the different superplasticizers was proportional to the total number of carboxylate units (or number of repeating units times the repeat unit charge density). They discovered that the dependence was equal for both addition modes with the notable difference that the hydration retardation below a critical dosage of the PCE (c^*) was very limited. They derived quantitative expressions to correlate the hydration retardation (Δt) and the structure of the comb-shaped copolymers for both addition modes as follows:

$$\text{Delayed addition } \Delta t \propto n_{RU}^{tot}\left(\frac{C/E}{C/E+1}\right)^{3/2} \quad (5)$$

$$\text{Direct addition } \Delta t \propto \left(n_{RU}^{tot} - n_{RU}^{Ett}\right)\left(\frac{C/E}{C/E+1}\right)^{3/2} \quad (6)$$

where, Δt is the hydration retardation (in hour), $n_{RU}^{tot} = \frac{c_{PCE}}{M_{RU}}$ is the number of repeat units dosed in the system, n_{RU}^{Ett} is the number of repeat units adsorb in ettringite, c_{PCE} is the concentration of PCE in $\mu g_{PCE} \cdot g_{OPC}{}^{-1}$, M_{RU} the molar mass of a repeat unit defined in Equation 7 (g mol^{-1}), and C/E (or N) the molar ratio of MAA/PEGMA.

$$M_{RU} = P \cdot M_{SC} + (C/E+1) \cdot M_{BB} \quad (7)$$

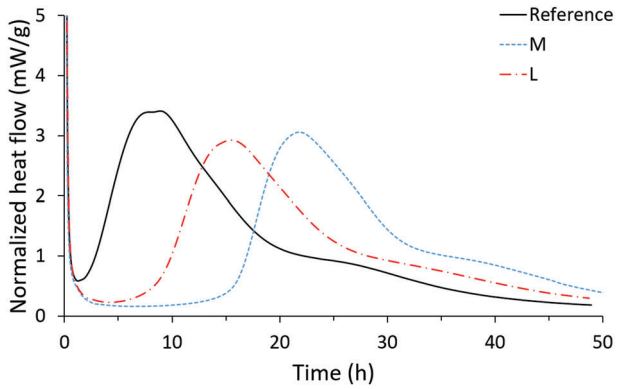

Figure 7. Effect of the side chain length of the PCE at 3 $mg_{PCE} \cdot g_{OPC}^{-1}$ concentration and 3/1 MAA/PEGMA ratio.

where M_{RU} is the molar mass of the repeating unit, P the side chain length, M_{SC} the molar mass of the side chain (ethylene oxide, 44.05 g mol^{-1}), $(C/E + 1)$ the number of monomer units in the repeating unit, and M_{BB} the molar mass of the backbone monomer (MAA, 86.06 g mol^{-1})

The fact that the experimental retardation observed in both addition modes showed a similar dependence on the molecular structure suggested to the authors that the same mechanism was involved in the retardation of the hydration. The authors, and for the first time, experimentally demonstrated that among the potential competing mechanisms that might explain the retardation of silicate hydration by PCEs, the reduction of the dissolution of the tricalcium silicate was the most probable. They concluded that dissolution is the rate-limiting step for silicate hydration and that PCEs delay it by blocking reactive dissolution areas (e.g., areas of higher density of kinks, such as for example, corners and etch pits, which are the most reactive areas in surfaces) that would otherwise develop as dissolution pits and retreating steps.

Furthermore, the authors rationalized the dependence of the delay of the hydration on the structural properties of the comb-like copolymers presented in Equations 5 and 6 using first principle considerations. Thus, they explained that the dependences in Equations 5 and 6 can be seen as the product between the number of added repeat units, n_{RU}^{tot}, or $(n_{RU}^{tot} - n_{RU}^{Ett})$ (which are linked to the surface coverage or the adsorption capacity of the polymers) and the blocking capacity of each repeated unit, $(\frac{C/E}{C/E+1})^{3/2}$, which depends on the electric field induced by the polymer on the surface.

In this work, we assess these dependencies for PCE's synthesized by aqueous free-radical copolymerization for hydration kinetics obtained in the direct addition mode. First, as presented by Marchon et al., the retardation of the maximum of the hydration curve (Δt, taken from the data of the calorimetric measurements in the Supporting Information (Section 4)) was plotted as a function of the quantity of carboxylate groups (x_0) calculated with Equation 8 (**Figure 8**).

$$x_0 = c_{PCE} \cdot \frac{C/E}{M_{RU}} \tag{8}$$

Figure 8, in agreement with the results of Marchon et al.,[5] shows that the delay time for the hydration increases linearly with the molar quantity of carboxylate groups in the PCE and it is independent of the side chain length (P).

Then, we plot Δt as function $n_{RU}^{tot}(\frac{C/E}{C/E+1})^{3/2}$(**Figure 9**) to validate whether the master curves obtained by Marchon et al.[5] hold for PCEs synthesized by free-radical copolymerization (with the characteristic structural parameters determined by AF4/MALS/RI and ^{1}H and ^{13}C NMR) and for their effect on the hydration of a commercial OPC (with a composition far from the model clinker used in their work). Tables 2 and 3 are for details and legend.

Figure 9 shows a reasonable linear dependence and hence validates the dependence proposed by Marchon et al.[5] (Equations 5 and 6) for comb-like copolymers synthesized by free radical copolymerization.

It is interesting that the dependence of Equation 5 obtained for delayed addition for a model clinker by Marchon et al. also holds here when the PCE is added in direct addition. In the case of direct addition, Marchon et al. found a nonlinear relationship for the same plot. The explanation provided by the authors is that up to a critical concentration (c^*) the PCE is adsorbed on the quickly formed ettringite phase and not in the tricalcium silicate and hence almost no delay is observed. Worth noting is that the composition of the model clinker used in Marchon's work is richer in aluminates than the OPC used in this work (17.2 wt.% vs 6.8 wt.%) and therefore, the impact of adsorption of PCE on ettringite is expected to be negligible. This simple explanation is corroborated by the XRD spectra and the specific surface areas measured over samples whose hydration process were stopped at 30 min (see Section S5, Supporting Information). On the one hand, the addition of PCE diminishes the early formation of specific surface area with respect to samples without superplasticizer. On the other hand, the XRD patterns clearly illustrate that the main peak of ettringite (≈9°) is less intense in the sample with PCE. Altogether, these evidences discard the promotion of ettringite nucleation and explain the linear dependence of the hydration delay with the concentration of PCE.

4. Conclusion

In this work, PCEs with uniform composition and different molecular architectures were synthesized by free-radical copolymerization varying the MAA/PEGMA ratios and ethylene oxide units in the PEGMA macromonomers. The homogeneity of the composition was assessed by ^{1}H-NMR and ^{13}C-NMR, while the molar mass distribution was measured by Asymmetric-Flow Field-Flow Fractionation, to obtain a full characterization of the microstructure of the PCEs.

Later, the effect of direct addition in the mixing water of these copolymers on the hydration kinetics of a commercial Ordinary Portland Cement (OPC) was analyzed by isothermal calorimetry. It was observed that by increasing the PCE concentration the hydration was delayed. Moreover, for a given PCE concentration, the delay was longer as the MAA/PEGMA ratio increased or the side chain length of the PEGMA decreased. Interestingly, contrary to what expected, the hydration delays of all the PCEs were found to be proportional to the carboxylate dosage. In fact, the delays fitted well with the master curve proposed in the state of the art for delayed additions. The explanation relies on the content of

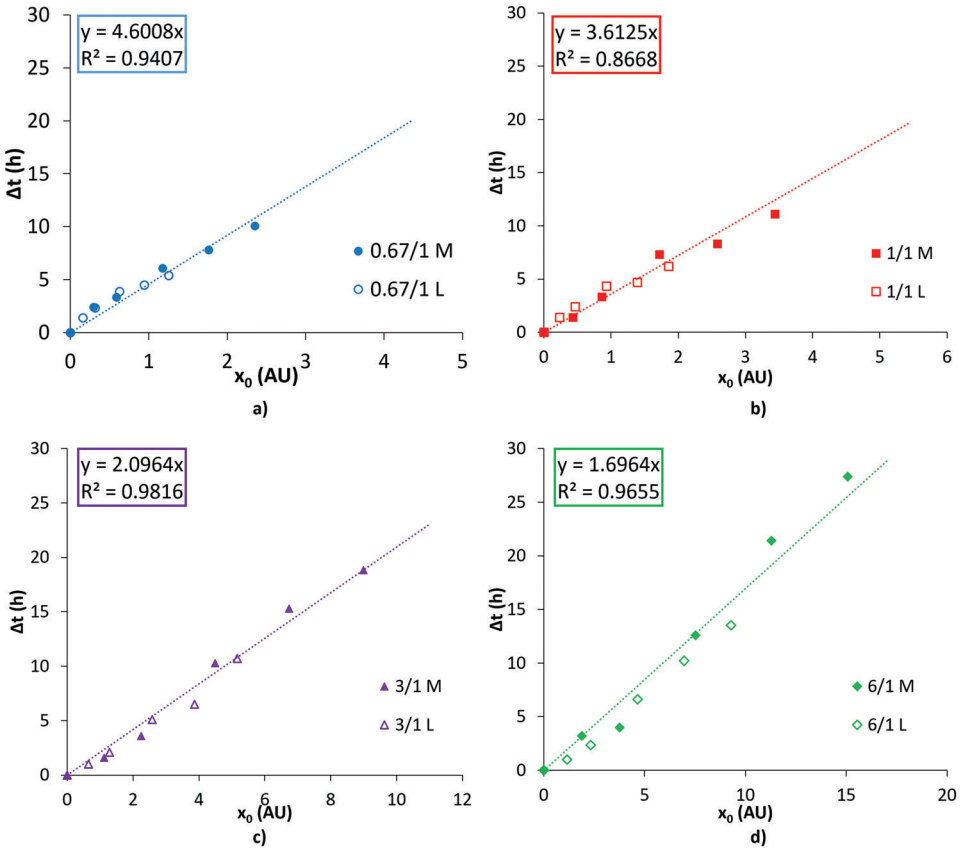

Figure 8. Retardation of the maximum of the hydration curve as a function of the dosage of carboxylic groups (in direct addition) for PCE's with different MAA/PEGMA mol ratios: a) 0.67/1, b) 1/1, c) 3/1, and d) 6/1.

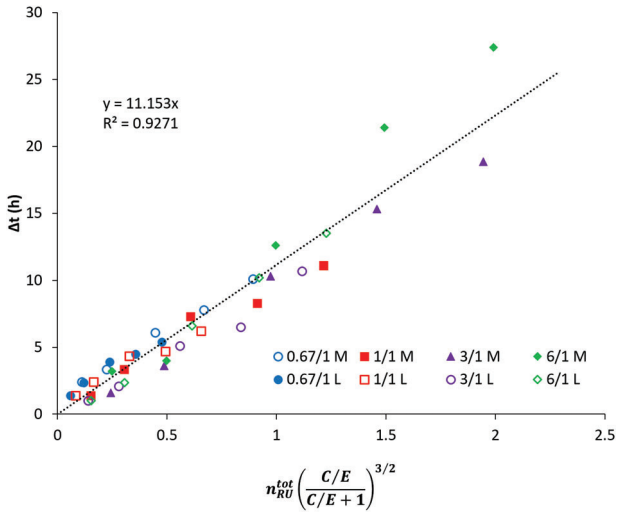

Figure 9. Master curve that shows that the delay is proportional to the number of repeating units ($\frac{c_{PCE}}{M_{RU}}$) and function of the polymer structure defined as $(\frac{\frac{C}{E}}{\frac{C}{E}+1})^{3/2}$.

C_3A and the lower role of ettringite for competing for the PCEs adsorption. More research will be carried out in near future to investigate the delayed addition for the same system along with exploring new cement compositions.

Supporting Information

Supporting Information is available from the Wiley Online Library or from the author.

Acknowledgements

The financial support from Eusko Jaurlaritza (GV-IT-1512-22), Ministerio de Ciencia e Innovación (PID2021-123146OB-I00) and LTC Green Concrete is gratefully acknowledged. Sara Beldarrain thanks the scholarship for master grants of POLYMAT.

Conflict of Interest

The authors declare no conflict of interest.

Data Availability Statement

The data that support the findings of this study are available from the corresponding author upon reasonable request.

Keywords

free-radical copolymerization, microstructure, hydration, ordinary portland cement, polycarboxylate ether

Received: January 30, 2023
Revised: March 10, 2023
Published online: April 21, 2023

[1] J. Plank, E. Sakai, C. W. Miao, C. Yu, J. X. Hong, *Cem. Concr. Res.* **2015**, *78*, 81.
[2] C. Schröfl, M. Gruber, J. Plank, *Cem. Concr. Res.* **2012**, *42*, 1401.
[3] M. Benaicha, A. Hafidi Alaoui, O. Jalbaud, Y. Burtschell, *J. Mater. Res. Technol.* **2019**, *8*, 2063.
[4] R. J. Flatt, I. Schober, E. Raphael, C. Plassard, E. Lesniewska, *Langmuir* **2009**, *25*, 845.
[5] D. Marchon, P. Juilland, E. Gallucci, L. Frunz, R. J. Flatt, *J. Am. Ceram. Soc.* **2017**, *100*, 817.
[6] W. S. Price, *Ann. Rep. NMR Spectrosc.* **1999**, *38*, 289.
[7] I. Emaldi, A. Agirre, A. Etxeberria, E. Erkizia, J. Dolado, J. R. Leiza, *Macrom. React. Eng.* **2020**, *14*, 2000015.
[8] B. L. Smith, J. Klier, *J. Appl. Polym. Sci.* **1998**, *68*, 1019.
[9] C. Gay, E. Raphaël, *Adv. Colloid Interface Sci.* **2001**, *94*, 229.
[10] D. Marchon, F. Boscaro, R. J. Flatt, *Cem. Concr. Res.* **2019**, *115*, 116.
[11] F. Winnefeld, S. Becker, J. Pakusch, T. Götz, *Cem. Concr. Compos.* **2007**, *29*, 251.
[12] A. Zingg, F. Winnefeld, L. Holzer, J. Pakusch, S. Becker, R. Figi, L. Gauckler, *Cem. Concr. Compos.* **2009**, *31*, 153.
[13] Q. Ran, P. Somasundaran, C. Miao, J. Liu, S. Wu, J. Shen, *J. Colloid Interface Sci.* **2009**, *336*, 624.
[14] A. Kauppi, K. M. Andersson, L. Bergström, *Cem. Concr. Res.* **2005**, *35*, 133.

